



# Pumping with Modified Polyurethane Sponges: A Rapid Oil Spill Treatment Technology

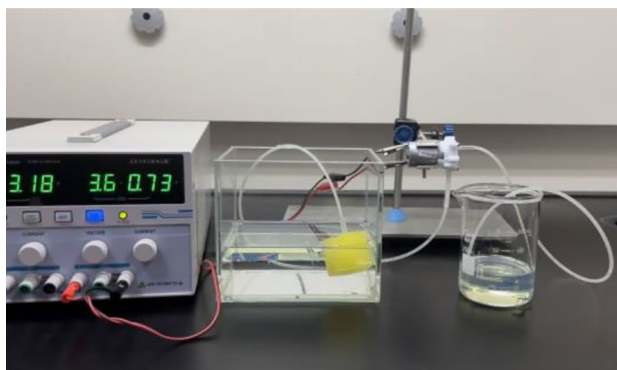
Yupu Meng<sup>1</sup> · Xiaohong Zhou<sup>1</sup> · Zhiwei Huang<sup>1</sup> · Zhuqing Wang<sup>1</sup>

Received: 8 December 2023 / Revised: 31 January 2024 / Accepted: 18 February 2024 / Published online: 28 February 2024  
© The Author(s), under exclusive licence to Korean Institute of Chemical Engineers, Seoul, Korea 2024

## Abstract

With the rapid development of the marine transportation and oil exploration industries, oil spill accidents, such as ship discharges and leakages from oil transport vessels and offshore drilling platforms, occur from time to time, turning oil spill pollution at sea into an increasingly serious problem. Therefore, developing a rapid and efficient oil spill pollution treatment is of great significance to protect the water environment. In this study, we used a simple dip-coating method to modify polydimethylsiloxane and nano-alumina onto a polyurethane sponge skeleton to prepare a super-oleophilic/super-hydrophobic porous adsorbent called  $\text{Al}_2\text{O}_3@\text{PDMS/PU}$ . The prepared  $\text{Al}_2\text{O}_3@\text{PDMS/PU}$  has a contact angle of  $156.8^\circ$  with water and can adsorb oil or organic solvents equivalent to 16–38 times its own weight. Based on the excellent super-oleophilic/super-hydrophobic properties of  $\text{Al}_2\text{O}_3@\text{PDMS/PU}$ , we designed an oil collection device that can continuously recover oil and organic solvents. Unlike the traditional oil recovery method, this device integrates the oil–water separation and oil recovery processes such that the adsorption capacity of the adsorbent is no longer limited by its own weight and volume. This device shows broad application prospects in emergencies, such as oil leakages from drilling platforms and organic solvent leakage.

## Graphical Abstract



Oil collection device for efficient recovery of oil in situ

**Keywords** Oil–water separation · Adsorbent · Super lipophilic · Oil-collecting device · Polyurethane sponge

## Introduction

Fuel oil and organic solvents play an important role in human activities and social production. However, the leakage of oil and organic solvents during transportation and use not only brings economic losses but also seriously damages the ecological environment, thus negatively affecting the survival of wild animals and plants and sailing and fishing

✉ Zhuqing Wang  
wangzhq@aqnu.edu.cn

<sup>1</sup> Anhui Key Laboratory of Photoelectric-Magnetic Functional Materials, Anqing Normal University, Anqing 246133, China

activities. The discharge of organic polluted wastewater (e.g., brine) also degrades the quality of water to levels that are no longer safe for consumption (via desalination) and industrial applications [1–6]. Therefore, an efficient recovery of leaked oil or organic solvents is of great significance [7, 8].

Among the most commonly used treatment methods for oil spills and organic solvent leaks at home and abroad include in situ combustion, mechanical extraction, biodegradation, chemical methods, and adsorption methods [9–12]. Despite its easy operation, the in situ combustion method releases toxic gases, such as CO, SO<sub>2</sub>, and polycyclic aromatic hydrocarbons, into the atmosphere, thus generating secondary pollution. The mechanical extraction method has a large processing capacity and does not cause secondary pollution, but the required device is large in size and has a cumbersome operation, making it unsuitable for responding to emergencies. Biodegradation is time consuming and easily affected by the environment, whereas chemical treatment easily produces toxic gases. Adsorption has attracted increasing application in recent years due to its recycling of oil absorption materials, limited generation of secondary pollution, low technical requirements, and low cost [13–15]. When treating oil spills, adsorption often uses oil booms to control the oil slick on the water surface, covers them with oil absorption materials, and then collects these materials via mechanical extrusion or vacuum distillation. However, during the treatment process, the adsorption and separation steps are conducted separately, thus requiring many operating steps and consuming much time and labor. In addition, mechanical extrusion or vacuum distillation operations damage the structure of oil-absorbing materials, thus reducing their oil-absorbing performance after repeated use [16–18]. Therefore, developing an in situ adsorption/desorption oil-absorbing material and a sustainable oil spill recovery device is of great significance [19–21].

The most commonly used oil-absorbing materials today include activated carbon, cotton fiber, vermiculite, artificial polymers, turpentine, and bentonite [22, 23]. These materials have two commonalities, one is that their surfaces are lipophilic/hydrophobic, and the other is that they have a 3D porous structure, which is convenient for the adsorption and storage of oil. Among them, artificial polymer polyurethane sponge has become an ideal oil–water separation material due to its high resilience, low density, high absorption capacity, and easy large-scale production [24, 25]. Professor Yang Wenjie et al. [26] modified a polyurethane sponge with expanded graphite and zinc oxide, and the prepared modified polyurethane sponge demonstrated good lipophilic/hydrophobic properties with a contact angle of 134°. Professor Wu Tao et al. [27] modified a super-hydrophobic sepiolite on a 3D porous polyurethane sponge skeleton, and the contact angle of the modified polyurethane sponge material to

water reached 148°. However, in experiments using modified polyurethane sponges as adsorbents to clean oil spills on water surfaces, the removal of oil and the reusability of adsorbents received limited research attention [28]. Mechanical extrusion and vacuum distillation consume much time and can easily damage the sponge structure, thus reducing its oil–water separation ability [29, 30]. Zhu Haitao et al. [31] built an emergency oil collection device where an oil-absorbing sponge was connected to a self-priming pump in order for the adsorbent to efficiently recover oil without being limited by adsorption capacity. However, this adsorbent has a complex preparation process and limited practicality.

Inspired by the superhydrophobic properties of the lotus leaf (surface concave and convex structure and ultra-low surface energy), we use polydimethylsiloxane (PDMS) with ultra-low surface energy and nano-Al<sub>2</sub>O<sub>3</sub> as modifiers to modify the polyurethane sponge with a 3D porous structure to prepare a super-oleophilic/super-hydrophobic modified sponge material called Al<sub>2</sub>O<sub>3</sub>@PDMS/PU. Relying on the excellent oil absorption performance of this material, we also develop a set of devices for recovering oil (e.g., diesel oil and petroleum crude oil) and organic solvents (e.g., n-hexane and carbon tetrachloride) on the water surface. We also discuss the effects of working voltage, oil viscosity, nozzle height, working time, and other experimental parameters and the adsorption/desorption mechanism of Al<sub>2</sub>O<sub>3</sub>@PDMS/PU.

## Experimental

### Materials

n-Hexane, dichloromethane, carbon tetrachloride, petroleum ether, methylene blue, oil red O, methylene blue, and nano-Al<sub>2</sub>O<sub>3</sub> (20 nm) were purchased from Aladdin Chemical Reagent Company (Shanghai, China). Sylgard 184 polydimethylsiloxane (PDMS) and the curing agent were purchased from Dow Corning (Midland, USA). Diesel, petroleum crude oil, and engine oil (20–40 W) were provided by the China Petroleum & Chemical Corporation Anqing Branch. Rapeseed oil and sunflower oil were purchased from Carrefour Supermarket (Anqing, Anhui). A self-priming pump (RS-360SH) and polytetrafluoroethylene tube (inner diameter 2 mm, outer diameter 3 mm) were purchased from Maker Storm Studio (Shenzhen, China). The polyurethane sponge was purchased from the Zhiyue store on JD.com, China.

## Instrument

The morphology, structure, and element distribution of the materials were photographed by a Regulus 8600 field emission scanning electron microscope (Hitachi, Japan), whereas their chemical composition and functional groups were determined by a Nicolet iS50 Fourier transform infrared spectrometer (Thermo Fisher Company, USA). The contact angle data of the sponge raw materials, PDMS-PU, and  $\text{Al}_2\text{O}_3$ @PDMS/PU to water were measured by the DSA100 contact angle measuring instrument (KRUSS, Germany). A JK-700DB ultrasonic cleaner (Hefei Jinnick Machinery Manufacturing Co., Ltd., China) was used to clean the polyurethane sponge and disperse the nano- $\text{Al}_2\text{O}_3$  particles.

## Preparation of $\text{Al}_2\text{O}_3$ @PDMS/PU

Large pieces of polyurethane sponge were cut into small pieces of about  $3 \times 3 \times 3$  cm, cleaned with water in an ultrasonic cleaner, and dried for later use. Under magnetic stirring, 2.0 g PDMS and 0.2 g curing agent were successively added into a beaker filled with 75 mL n-hexane. After stirring evenly, 3.0 g nano- $\text{Al}_2\text{O}_3$  was added. After stirring for 5 min, the beaker was transferred to an ultrasonic cleaner for ultrasonic wave for 5 min. Afterward, the polyurethane sponge was soaked in the mixed solution and extruded with a glass rod to discharge the air in the sponge. After 3 min, the sponge was taken out and naturally dried in a clean Petri dish for 4 h. The sponge was then dried in an oven at 80 °C for 2 h to obtain the final  $\text{Al}_2\text{O}_3$ @PDMS/PU.

## Adsorption Capacity ( $M$ ), Oil–Water Separation Efficiency ( $\eta$ ), and Oil Flux of the Device ( $J$ )

The adsorption capacity ( $M$ , g/g) and oil–water separation efficiency ( $\eta$ , %) of  $\text{Al}_2\text{O}_3$ @PDMS/PU for different oil materials were calculated using formulas (1) and (2), respectively, and the oil flux ( $J$ ,  $\text{L m}^{-2} \text{h}^{-1}$ ) of the device was calculated using the formula (3):

$$M = \frac{w_i - w_o}{w_o}, \quad (1)$$

$$\eta = \left(1 - \frac{V_1}{V_o}\right) \times 100\%, \quad (2)$$

$$J = \frac{V}{A \times T}, \quad (3)$$

where  $w_o$ (g) is the mass of  $\text{Al}_2\text{O}_3$ @PDMS/PU before adsorbing oil,  $w_i$ (g) is its mass after adsorbing oil (e.g., diesel, petroleum crude oil, engine oil, rapeseed oil, petroleum ether, or carbon tetrachloride),  $V_o$ (L) is the total volume after mixing dichloromethane and water (1:1),  $V_1$ (L) is the

volume of remaining water,  $V$ (L) is the total volume of oil collected by the device,  $A$ (m) is the contact area between  $\text{Al}_2\text{O}_3$ @PDMS/PU and oil, and  $T$ (h) is the time required to collect oil.

## Oil Collection Device

The oil collection device consists of four parts, namely, the core material  $\text{Al}_2\text{O}_3$ @PDMS/PU, self-priming pump, stabilized DC power supply, and conduit. One end of one catheter was inserted into  $\text{Al}_2\text{O}_3$ @PDMS/PU, and the other end was connected to the inlet of the micro self-priming pump. One end of the other catheter was connected to the outlet of the self-priming pump, and the other end was placed in an oil collection container (beaker). The self-priming pump and DC-regulated power supply were connected with wires. After setting the working voltage, the regulated power supply switch was turned on to begin the operation.

## Results and Discussion

### Materials' Characterization

To determine whether PDMS was successfully modified on the surface of the polyurethane sponge material, we conducted an infrared spectral characterization of the raw material PU and  $\text{Al}_2\text{O}_3$ @PDMS/PU. As shown in Fig. 1a, the absorption peak at  $2966 \text{ cm}^{-1}$  can be attributed to the symmetric stretching vibration of the C–H bond in  $-\text{CH}_3$ , while the absorption peaks at  $1712 \text{ cm}^{-1}$  and  $1639 \text{ cm}^{-1}$  can be attributed to the stretching vibration of C=O and C=C bonds, respectively, thus indicating that the surface of

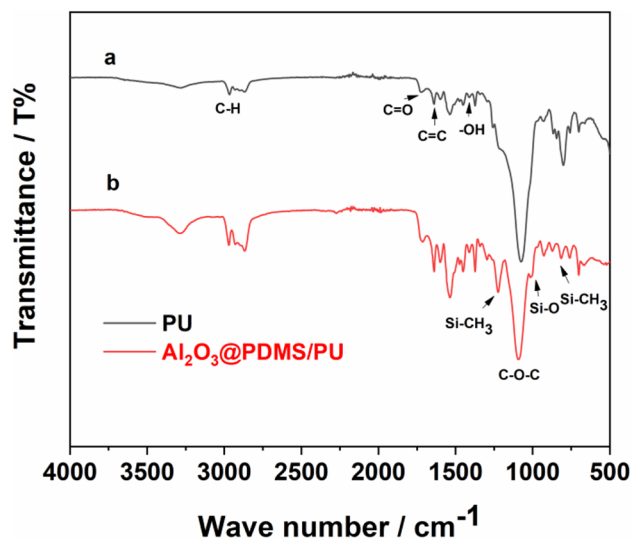


Fig. 1 Infrared spectra of PU and  $\text{Al}_2\text{O}_3$ @PDMS/PU

the PU material contains furan groups and aromatics. The absorption peak at  $1410\text{ cm}^{-1}$  may be the characteristic peak of the deformation vibration of  $-\text{OH}$ , and the absorption peak at  $1087\text{ cm}^{-1}$  may be caused by the stretching vibration of  $-\text{C}-\text{O}-\text{C}-$ . Compared with the PU sponge,  $\text{Al}_2\text{O}_3@$ PDMS/PU has new bending vibration and stretching vibration peaks of  $\text{Si}-\text{CH}_3$  at  $1223\text{ cm}^{-1}$  and  $814\text{ cm}^{-1}$ . The new absorption peak at  $1006\text{ cm}^{-1}$  can be attributed to the  $\text{Si}-\text{O}$  vibration (Fig. 1b). These new absorption peaks indicate that PDMS was successfully grafted onto the PU sponge skeleton.

We used the BET method to test the specific surface area of PU and  $\text{Al}_2\text{O}_3@$ PDMS/PU and then drew the adsorption and desorption isotherms. After loading nano- $\text{Al}_2\text{O}_3$ , the specific surface area of  $\text{Al}_2\text{O}_3@$ PDMS/PU increased from  $1.04$  to  $4.2\text{ m}^2/\text{g}$  due to the large amount of nano- $\text{Al}_2\text{O}_3$

loaded on the sponge surface, thus increasing its surface roughness (refer to the SEM images of PU and  $\text{Al}_2\text{O}_3@$ PDMS/PU). PU and  $\text{Al}_2\text{O}_3@$ PDMS/PU present type III isotherms, thus confirming their macroporous structures (Fig. 2). Therefore, compared with PU,  $\text{Al}_2\text{O}_3@$ PDMS/PU can wet, adsorb, and store oil easier.

As shown in Fig. 3, PU, PDMS/PU, and  $\text{Al}_2\text{O}_3@$ PDMS/PU have 3D macropore structures, which are beneficial to the storage and movement of oil. According to the Cassie-Baxter model (i.e., under the condition of the same surface energy, a rough surface can provide better hydrophobic properties than a smooth surface), to improve hydrophobicity, we further modified the PDMS/PU material (Fig. 3b) by grafting nano- $\text{Al}_2\text{O}_3$  particles to change its surface morphology. Figure 3c shows that the prepared  $\text{Al}_2\text{O}_3@$ PDMS/PU has an uneven surface similar to that of a lotus leaf, whereas its

**Fig. 2**  $\text{N}_2$  adsorption–desorption isotherm of **a** PU and **b**  $\text{Al}_2\text{O}_3@$ PDMS/PU

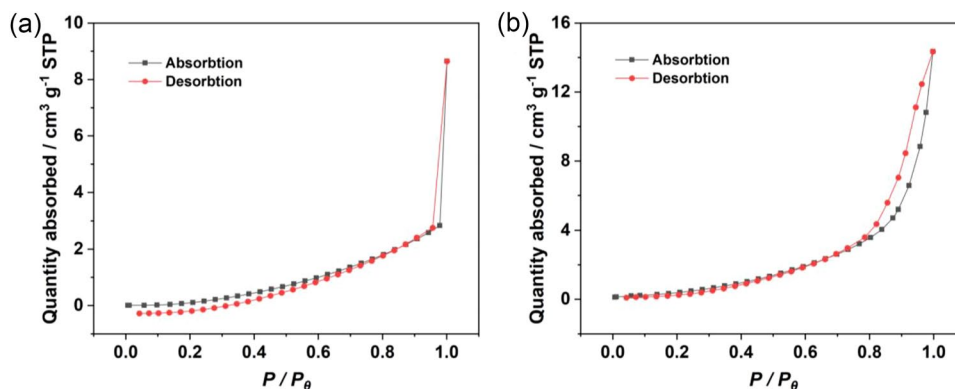
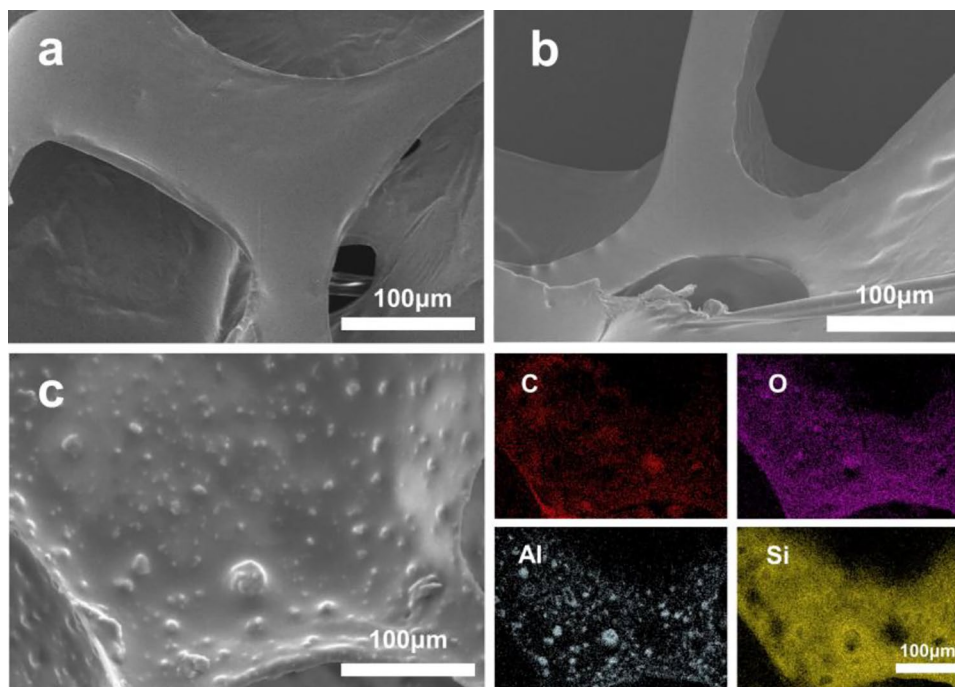


**Fig. 3** SEM images of **a** PU and **b** PDMS/PU. **c** SEM image and EDS mapping image of  $\text{Al}_2\text{O}_3@$ PDMS/PU



water contact angle reaches  $156.8^\circ$  [32]. The X-ray energy spectrum analysis show that carbon (C), oxygen (O), aluminum (Al), and silicon (Si) elements are uniformly distributed on the surface of  $\text{Al}_2\text{O}_3@\text{PDMS}/\text{PU}$ .

As shown in Fig. 4, the water contact angles of PU, PDMS/PU, and  $\text{Al}_2\text{O}_3@\text{PDMS}/\text{PU}$  are  $131.9^\circ$ ,  $141.3^\circ$ , and  $156.8^\circ$ , respectively, and the water droplets show a perfect spherical shape on  $\text{Al}_2\text{O}_3@\text{PDMS}/\text{PU}$ . When  $\text{Al}_2\text{O}_3@\text{PDMS}/\text{PU}$  was immersed in water by an external force, the gas in the material produced a “mirror” at the interface between the material and water (Fig. 5a) that blocked the entry of water. Nevertheless,  $\text{Al}_2\text{O}_3@\text{PDMS}/\text{PU}$  could still automatically absorb oil or organic solvents (Fig. 5b). After the adsorption reached saturation,  $\text{Al}_2\text{O}_3@\text{PDMS}/\text{PU}$  could still float on the water surface, thus confirming its good lipophilic/hydrophobic properties. The adsorption experiment results of  $\text{Al}_2\text{O}_3@\text{PDMS}/\text{PU}$  on different oils confirm that this material can adsorb oils or organic solvents equivalent to 16–38 times its own weight (Fig. 5c). These characteristics increase the application prospects of this material in oil storage and transportation.

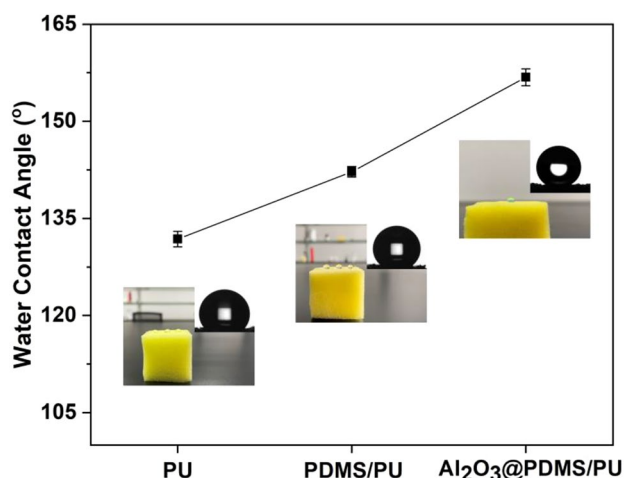
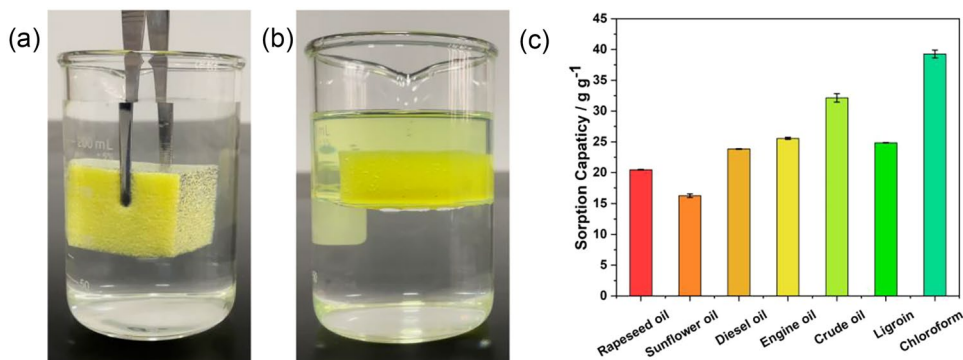


Fig. 4 Contact angles of PU, PDMS/PU, and  $\text{Al}_2\text{O}_3@\text{PDMS}/\text{PU}$  to water

Fig. 5 **a**  $\text{Al}_2\text{O}_3@\text{PDMS}/\text{PU}$  is immersed in water. **b**  $\text{Al}_2\text{O}_3@\text{PDMS}/\text{PU}$  is placed in an oil–water mixture. **c**  $\text{Al}_2\text{O}_3@\text{PDMS}/\text{PU}$  adsorption capacity for different oil materials



The reusability of oil–water separation materials is an important parameter for evaluating their performance. Diesel, crude oil, and  $\text{CCl}_4$  were selected in this experiment to test the reusability performance of  $\text{Al}_2\text{O}_3@\text{PDMS}/\text{PU}$ . First,  $\text{Al}_2\text{O}_3@\text{PDMS}/\text{PU}$  was placed in the liquid and taken out after fully absorbing the oil or organic solvent. The adsorption capacity  $M$  of the material was then computed using formula (1). Afterward, the adsorbed oil or organic solvent in the adsorbent was squeezed out by mechanical extrusion, the mass of the adsorbent after deoiling was measured again, and the above operation was repeated. As shown in Fig. 6, after ten times of repeated oil absorption and deoiling, the adsorption capacities of  $\text{Al}_2\text{O}_3@\text{PDMS}/\text{PU}$  for diesel, crude oil, and  $\text{CCl}_4$  were  $23.6 (\pm 0.96)$ ,  $32.7 (\pm 0.65)$ , and  $38.7 (\pm 0.38)$ , respectively. The adsorption capacity of  $\text{Al}_2\text{O}_3@\text{PDMS}/\text{PU}$  was also unchanged after multiple uses, indicating its good reusability in the oil–water separation process.

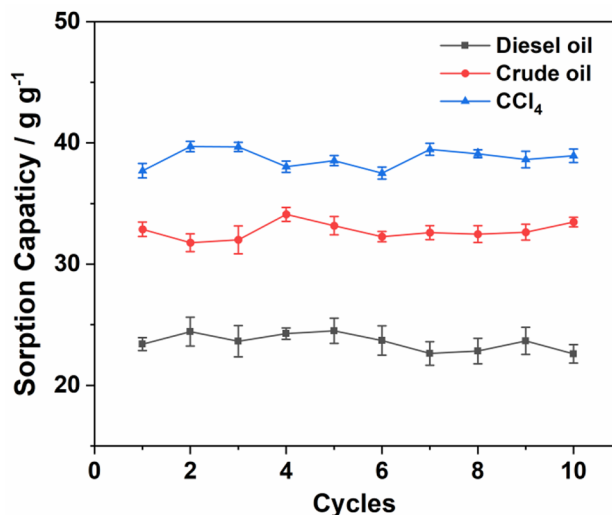


Fig. 6 Oil adsorption capacity of  $\text{Al}_2\text{O}_3@\text{PDMS}/\text{PU}$  after repeated use



We also tested the oil–water separation efficiency of  $\text{Al}_2\text{O}_3@\text{PDMS}/\text{PU}$  using the gravity separation method. As shown in Fig. 7, under the influence of gravity, the methylene chloride and water in the mixed solution passed through the unmodified PU. While the methylene chloride in the mixed solution quickly penetrated and passed through the  $\text{Al}_2\text{O}_3@\text{PDMS}/\text{PU}$ , the water was unable to pass through due to repulsion. Repeated test results show that the separation efficiency of dichloromethane/water by  $\text{Al}_2\text{O}_3@\text{PDMS}/\text{PU}$  remains above 99.4% ( $\pm 0.72$ ), thus confirming the good selectivity of this material to oils or organic solvents.

### Influence of Working Voltage

As shown in Fig. 8, as the operating voltage of the self-priming pump increased, the diesel recovery rapidly increased and then remained stable. When the voltage was below 2.0 V, the device could not efficiently separate the diesel fuel. When the voltage increased from 2.0 to 3.5 V, the recovery of diesel fuel rapidly increased, and when the operating voltage ranged from 3.5 to 4.0 V, the recovery of diesel fuel remained stable. When the voltage exceeded 4.0 V, bubbles started to form in the collected diesel fuel,

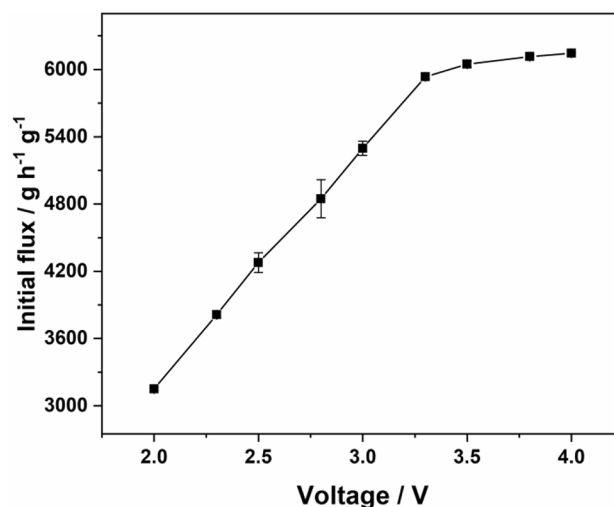


Fig. 8 Effect of voltage on diesel recovery rate of the device

thus indicating that the applied suction force is too large, causing air to enter the  $\text{Al}_2\text{O}_3@\text{PDMS}/\text{PU}$ . Therefore, to improve the recovery rate and save energy, the operating voltage was set to 3.5 V in this work.

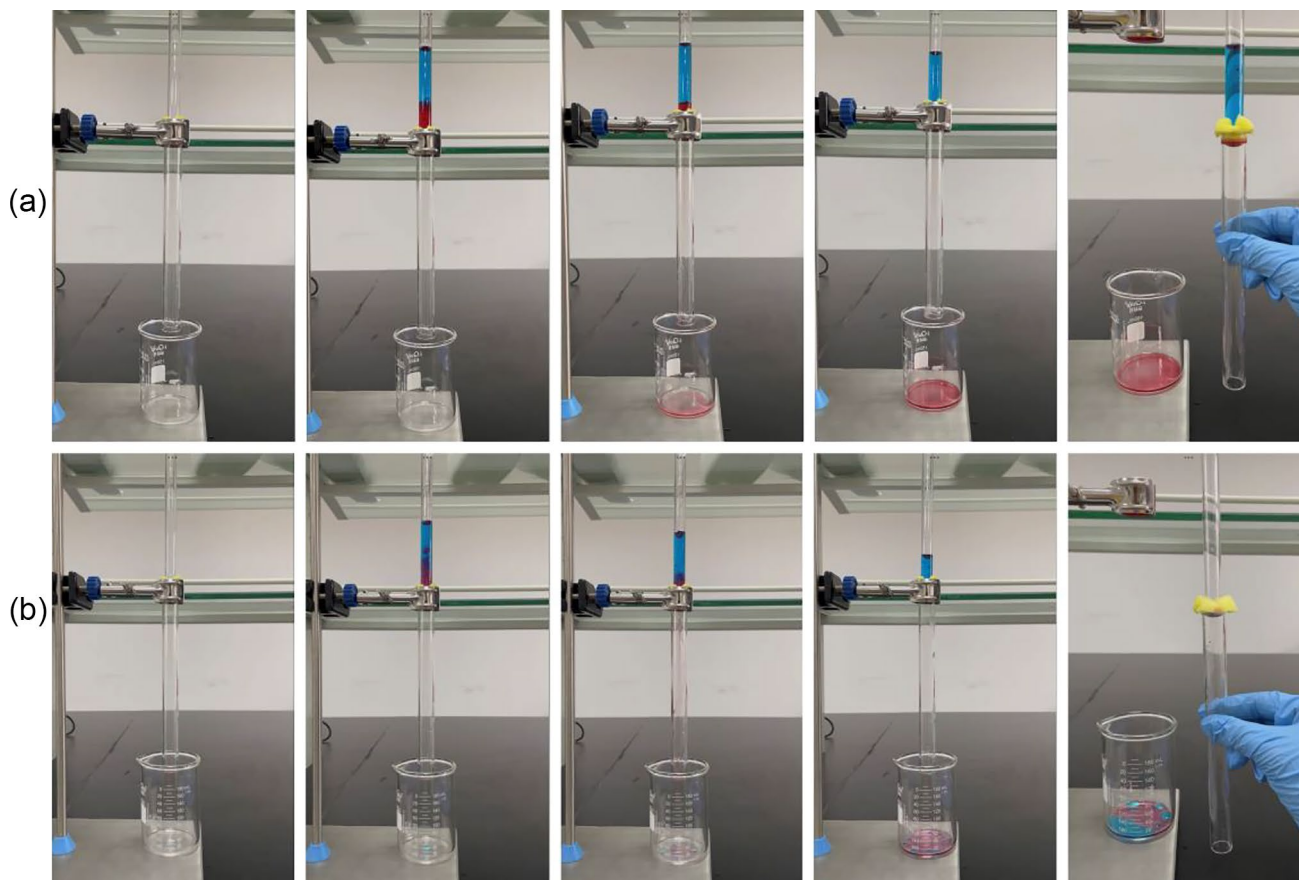


Fig. 7 **a**  $\text{Al}_2\text{O}_3@\text{PDMS}/\text{PU}$  separates dichloromethane/water mixture. **b** PU separates a dichloromethane/water mixture

### Influence of Oil Viscosity and Oil Suction Pipe Orifice Height

We also explored the impact of oil viscosity on unit recovery. By mixing *n*-hexane with engine oil in a volume ratio of 1:1, 1:2, 1:3, or 1:4, four oils with different viscosities were obtained, namely, *n*-hexane/engine oil-1 (66.8 CP), *n*-hexane/engine oil-2 (116.8 CP), *n*-hexane/engine oil-3 (152.6 CP), and *n*-hexane/engine oil-4 (171.9 CP). Under the same experimental conditions, Al<sub>2</sub>O<sub>3</sub>@PDMS/PU took 56, 82, 124, and 171 s to recover 60 mL of these oils, respectively. The experimental results are shown in Fig. 9. As the viscosity of the oil increased, the recovery efficiency of the oil collection device gradually decreased, consistent with Darcy’s law:

$$Q = \frac{-kA\Delta P}{\mu h},$$

where *Q* is the oil recovery (recovery rate),  $\mu$  is the viscosity of the oil, *h* is the height difference between the water surface and the mouth of the suction pipe, *k* is the permeability of Al<sub>2</sub>O<sub>3</sub>@PDMS/PU, *A* is the cross-sectional area of Al<sub>2</sub>O<sub>3</sub>@PDMS/PU, and  $\Delta P$  is the pressure difference at the mouth of the suction pipe. Given that  $\Delta P$  increases along with pump voltage, *Q* increases along with the self-priming pump operating voltage. On the contrary, as the oil viscosity increases, *Q* decreases.

In addition, we also explored the effect of the height difference between the oil suction pipe nozzle and the oil–water interface on the diesel recovery rate of the device. As shown in Fig. 10, the recovery rate of diesel oil decreased along with an increasing height difference between the oil suction

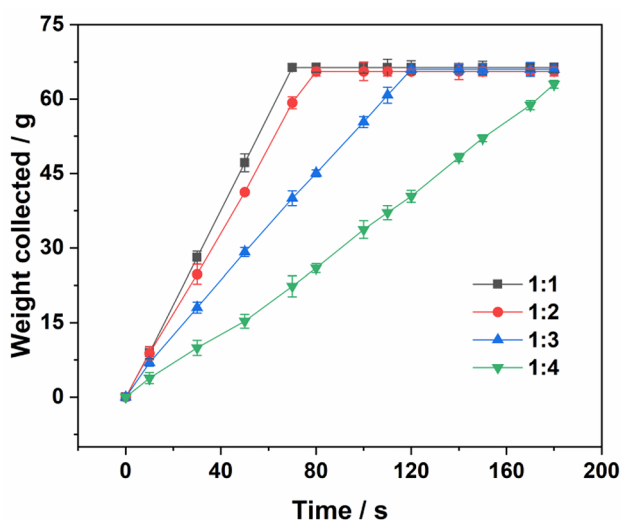


Fig. 9 Effect of viscosity on oil recovery

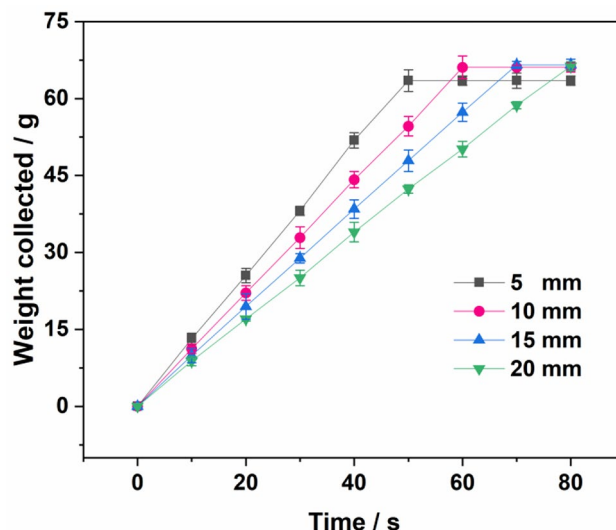


Fig. 10 Effect of suction pipe orifice height on oil recovery rate

pipe nozzle and the oil–water interface. Specifically, when the height difference was 20 mm, Al<sub>2</sub>O<sub>3</sub>@PDMS/PU took 72 s to recover 60 mL of diesel. When the height difference was 5 mm, the recovery took 48 s. These results also accord with Darcy’s Law. Therefore, to achieve maximum recovery under low energy consumption, the height of the suction pipe orifice and the oil–water interface should be kept consistent as much as possible.

### Application of Oil Collection Device

To verify the practicability of the proposed oil-collecting device, we used oil-collecting device to recover organic solvents and oil on the water surface. As shown in Fig. 11, our device efficiently recovered diesel fuel (Fig. 11a, Video S1), *n*-hexane (Fig. 11b, Video S2, with *n*-hexane colored by oil red O and water colored by methylene blue), and petroleum crude oil (Fig. 11d, Video S4) from the water surface. Due to its high viscosity, the collection efficiency for petroleum crude oil was relatively slow. Due to the excellent superhydrophobic/superoleophilic properties of Al<sub>2</sub>O<sub>3</sub>@PDMS/PU, this material selectively recovered underwater organic solvents, such as carbon tetrachloride (Fig. 11c, Video S3).

Unlike traditional oil spill repair methods, the oil-collecting device can absorb/desorb oil in situ, thus realizing an integration of adsorption and separation, which not only overcomes the limited oil absorption capacity of the sorbent blanket material but also avoids damage to the material structure caused by traditional mechanical extrusion and distillation operations. In addition, the device can also work for a long time (continuous operation for 18 h) and maintains a stable recovery rate (Fig. 12).

**Fig. 11** **a** Recovery of diesel on the water surface. **b** Recovery of n-hexane on the water surface. **c** Recovery of carbon tetrachloride underwater. **d** Recovery of petroleum crude oil on the water surface

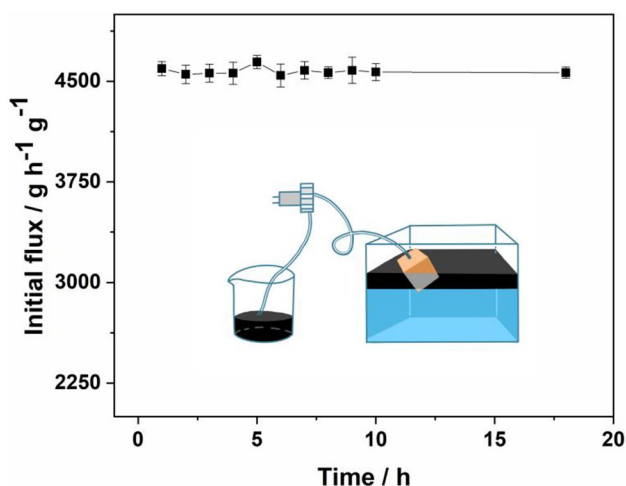
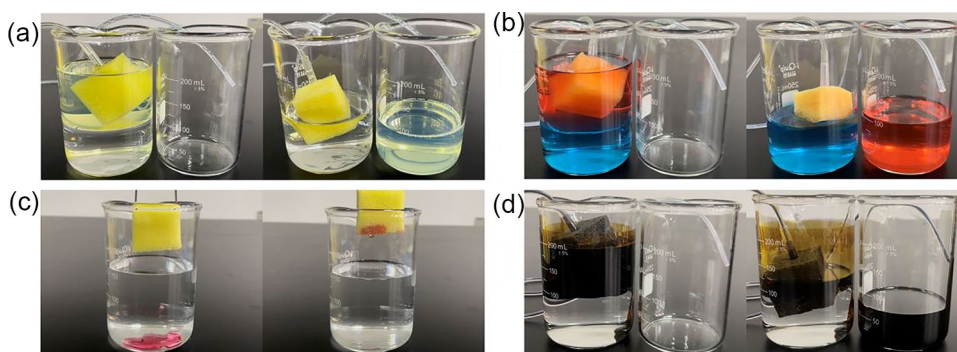


**Fig. 12** Effect of long-term operation of the oil collection device

We then compared the cost and performance of  $\text{Al}_2\text{O}_3$ @PDMS/PU with the oil–water separation materials and related devices published in the literature. As shown in

Table 1, the device developed in this study has strong advantages in terms of cost and oil flux.

### Working Principle of the Oil Collection Device

To better explain the process and working principle of oil adsorption/desorption in an oil gathering unit, we simplified the irregular porous structure of  $\text{Al}_2\text{O}_3$ @PDMS/PU, modeled it as a regular multi-bundle capillary (Fig. 13), and analyzed its capillary pressure in the working process. Before the self-priming pump applies suction, the capillary pressure at the oil–air interface on top of  $\text{Al}_2\text{O}_3$ @PDMS/PU can be expressed as:

$$P_s = \frac{2\gamma_{OA}\cos\theta_1}{R},$$

where  $P_s$  represents the capillary pressure,  $R$  represents the radius of the capillary tube,  $\gamma_{OA}$  represents the oil–air interfacial tension, and  $\theta_1$  represents the contact angle of oil in the tube.

**Table 1** Cost and performance of various materials and their devices for oil–water separation

Material used and its production cost ( $\text{g}^{-1}$ )	Water contact angle	N-hexane flux ( $\text{L m}^{-2} \text{h}^{-1}$ )	Device composition and cost ( $\text{\$}$ ) <sup>a</sup>	Ref
TiO <sub>2</sub> -PU, \$4.30	152.0°	70.0	Vacuum Pump, 98.41	[31]
LDPE/EPDM TPV, \$0.35	161.9°	–	Vacuum pump and Valve, 94.82	[33]
WM-SiO <sub>2</sub> /OTS, \$3.89	147.5°	1.49	Peristaltic pump and T-shaped glass tube, 463.42	[34]
PDMS-graphene sponges, \$3.10	126.6°	2.25	Vacuum Pump, 95.49	[35]
PGNW-T, \$4.40	154.4°	1.88	Vacuum pump and PP hollow tube, £ 97. 47	[36]
ER/RRPS/LSEC, \$1.58	152.5°	–	Peristaltic Pump, 452.43	[37]
UMS, \$2.55	139.0°	1.84	Vacuum Pump, 95.38	[38]
AW, \$1.03	155.1°	34.1	Peristaltic pump, Valve, and T-shaped connecting pipe, 268.01	[39]
CNT/PDMS-coated PU, \$2.71	162.0°	293.0	Vacuum Pump, 95.42	[40]
PDMS-CA, \$2.37	144.2°	121.0	Self-priming pump and power source, 53.27	[41]
$\text{Al}_2\text{O}_3$ @PDMS/PU, \$0.78	154.1°	175.1	Self-priming pump and power source, 44.07	Our work

<sup>a</sup>The default connection between the material and the pump is using PTEF pipes



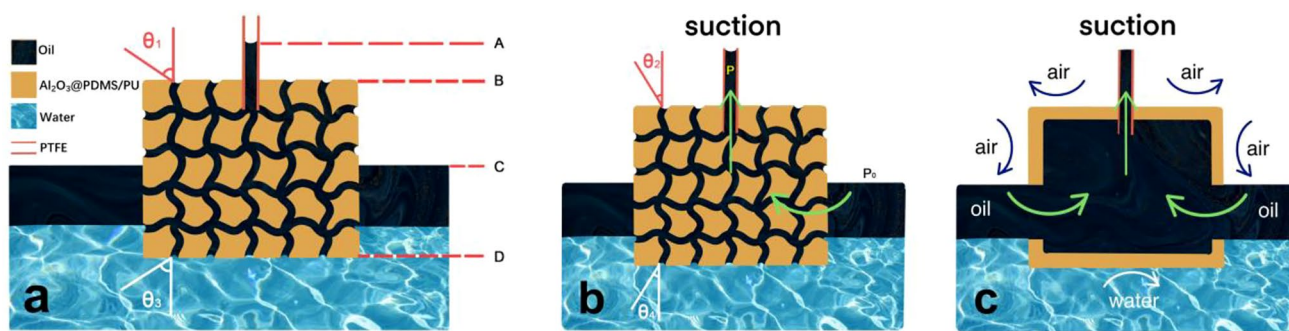


**Fig. 13** Schematic diagram of the self-priming pump **a** before and **b** after applying suction. **c** Schematic diagram of the self-controlled oil suction principle of  $\text{Al}_2\text{O}_3@PDMS/PU$

As shown in Fig. 13, after the self-priming pump applies suction, the capillary pressure ( $P_c$ ) on plane A increased as the contact angle decreased from  $\theta_1$  to  $\theta_2$ , and a new pressure balance was obtained between planes A and C. Therefore, air did not penetrate the oil–air interface of  $\text{Al}_2\text{O}_3@PDMS/PU$ . After applying suction, the capillary pressure at the bottom of  $\text{Al}_2\text{O}_3@PDMS/PU$  increased as the contact angle decreased from  $\theta_3$  to  $\theta_4$ . The increased capillary pressure at the oil–water interface and the superhydrophobic properties of the material surface can prevent water from penetrating into  $\text{Al}_2\text{O}_3@PDMS/PU$ . Given the absence of capillary pressure in plane C, after applying suction to  $\text{Al}_2\text{O}_3@PDMS/PU$ , the pressure balance between planes C and B was broken, and the pressure difference transported the oil from planes C to B.

Based on the above, the working principle of the device is illustrated in Fig. 13c, in which the oil–water and oil–air interfaces play a sealing role. After applying suction,  $\text{Al}_2\text{O}_3@PDMS/PU$  repelled water and air from entering its interior and only allowed floating oil to enter. Under the action of pressure difference, the oil flowed from planes C to B and was then discharged by the self-priming pump, thus achieving the purpose of oil–water separation and the recovery of oil on the water surface.

## Conclusion

In this study, we successfully prepared a super-lipophilic/super-hydrophobic  $\text{Al}_2\text{O}_3@PDMS/PU$  material by using a low-cost polyurethane sponge as raw material. The method has simple operation steps, a mature and reliable technical route, and can be produced on a large scale. The prepared  $\text{Al}_2\text{O}_3@PDMS/PU$  can efficiently adsorb oil or organic solvents 16–38 times its own weight and maintains a stable performance after 10 times of repeated use or 18 h of continuous oil separation. We also proposed a new oil collection device that can quickly and efficiently recover oil or

organic solvents with a dynamic viscosity range of 0–172 CP at a voltage of 3.5 V. This device is small in size, simple to operate, portable, has high oil recovery efficiency, can adsorb/desorb oil in situ, and realizes the integration of adsorption and separation. This device not only overcomes the limitation of oil absorption capacity on the adsorbent but also avoids damage to the material structure caused by traditional mechanical extrusion and distillation operations. Therefore, this new oil collection device not only alleviates environmental pollution but also reduces economic losses and provides an effective solution to oil spills or organic solvent leaks on the water surface.

**Supplementary Information** The online version contains supplementary material available at <https://doi.org/10.1007/s11814-024-00140-2>.

**Acknowledgements** This work was supported by the Anhui Provincial Department of Education (Nos. KJ2020A0493 and 2021jyxm0861).

**Data availability** The authors confirm that all data underlying the findings are fully available without restriction. All relevant data are within the paper.

## References

1. H.K. White, S.L. Lyons, S.J. Harrison, D.M. Findley, Y. Liu, E.B. Kujawinski, *Environ. Sci. Technol. Lett.* **1**, 295 (2014)
2. Y. Pi, N. Xu, M. Bao, Y. Li, D. Lv, P. Sun, *Environ. Sci.-Proc. Imp* **17**, 877 (2015)
3. M.L. Guarinello, S.K. Sturdivant, A.E. Murphy, L. Brown, J.A. Godbold, M. Solan, D.A. Carey, J.D. Germano, *ACS ES&T Water* **2**, 1760 (2022)
4. A. Panagopoulos, *Chem. Eng. Process. -Process Intensif.* **176**, 108944 (2022)
5. A. Panagopoulos, V. Giannika, *J. Environ. Manage.* **324**, 116239 (2022)
6. A. Panagopoulos, *Resource Recovery Ind. Waste Waters* **16**, 337 (2023)
7. P.C. Chen, Z.K. Xu, *Sci. Rep.* **3**, 2776 (2013)
8. M. Jin, J. Wang, X. Yao, M. Liao, Y. Zhao, L. Jiang, *Adv. Mater.* **23**, 2861 (2011)

9. R.S. Judson, M.T. Martin, D.M. Reif, K.A. Houck, T.B. Knudsen, D.M. Rotroff, M. Xia, S. Sakamuru, R. Huang, P. Shinn, C.P. Austin, R.J. Kavlock, D.J. Dix, *Environ. Sci. Technol.* **44**, 5979 (2010)
10. C.C. Brandão, A.C. Pinto Filho, *Water Sci. Technol. Sci. Technol.* **43**, 83 (2001)
11. Z. Chu, Y. Feng, S. Seeger, *Angew. Chem. Int. Ed. Engl.* **54**, 2328 (2015)
12. Z. Xue, Y. Cao, N. Liu, L. Feng, L. Jiang, *J. Mater. Chem. A* **2**, 2445 (2014)
13. W. Zheng, J. Huang, S. Li, M. Ge, L. Teng, Z. Chen, Y. Lai, *ACS Appl. Mater. Interfaces* **13**, 67 (2021)
14. X. Chen, J.A. Weibel, S.V. Garimella, *Ind. Eng. Chem. Res.* **55**, 3596 (2016)
15. X. Liu, L. Ge, W. Li, X. Wang, F. Li, *ACS Appl. Mater. Interfaces* **7**, 791 (2015)
16. Y. Liu, J. Ma, T. Wu, X. Wang, G. Huang, Y. Liu, H. Qiu, Y. Li, W. Wang, J. Gao, *ACS Appl. Mater. Interfaces* **5**, 10018 (2013)
17. L. Zhang, L. Xu, Y. Sun, N. Yang, *Ind. Eng. Chem. Res.* **55**, 11260 (2016)
18. F. Wang, S. Lei, C. Li, J. Ou, M. Xue, W. Li, *Ind. Eng. Chem. Res.* **53**, 7141 (2014)
19. W. Zhou, S. Li, Y. Liu, Z. Xu, S. Wei, G. Wang, J. Lian, Q. Jiang, *ACS Appl. Mater. Interfaces* **10**, 9841 (2018)
20. Z. Li, J. Qiu, S. Yuan, Q. Luo, C. Pei, *Ind. Eng. Chem. Res.* **56**, 6508 (2017)
21. J. Zhu, J. Hu, T. Peng, C. Jiang, S. Liu, Y. Li, T. Guo, L. Xie, *Adv. Mater. Interfaces Mater. Interfaces.* (2019). <https://doi.org/10.1002/admi.201900025>
22. Y. Wang, J. Knapp, A. Legere, J. Raney, L. Li, *RSC Adv.* **5**, 30570 (2015)
23. J. Zeng, Z. Guo, *Colloids Surf. A* **444**, 283 (2014)
24. C. Liu, S. Zhang, J. Li, J. Wei, K. Mullen, M. Yin, *Angew. Chem. Int. Ed. Engl.* **58**, 1638 (2019)
25. Y.C. Jung, B. Bhushan, *Langmuir* **25**, 14165 (2009)
26. C.B. Xu, L.K. Ma, Y. Zhao, W.J. Yang, *Res. Environ. Sci.* **29**, 1083 (2016)
27. S. Qiu, Y. Li, G. Li, Z. Zhang, Y. Li, T. Wu, *ACS Sustain. Chem. Eng.* **7**, 5560 (2019)
28. S.J. Choi, T.H. Kwon, H. Im, D.I. Moon, D.J. Baek, M.L. Seol, J.P. Duarte, Y.K. Choi, *ACS Appl. Mater. Interfaces* **3**, 4552 (2011)
29. Z. Lu, J. Song, K. Pan, J. Meng, Z. Xin, Y. Liu, Z. Zhao, R.H. Gong, J. Li, *ACS Appl. Mater. Interfaces* **11**, 20037 (2019)
30. J.L. Zhang, H. Xu, J. Guo, T.C. Chen, H.T. Liu, *Appl. Sci.-Basel* **10**, 13 (2020)
31. D. Wu, Z. Yu, W. Wu, L. Fang, H. Zhu, *RSC Adv.* **4**, 53514 (2014)
32. E. Ozkan, A. Mondal, P. Singha, M. Douglass, S.P. Hopkins, R. Devine, M. Garren, J. Manuel, J. Warnock, H. Handa, *ACS Appl. Mater. Interfaces* **12**, 51160 (2020)
33. X. Zhang, R. Feng, J. Wang, W. Wang, J. Hua, Z. Wang, *Macromole. Mater. Eng.. Mater. Eng.* (2021). <https://doi.org/10.1002/mame.202000745>
34. L. Ning, Y. Liu, Y. Luo, Y. Han, L. Zhang, M. Zhang, *Environ. Sci.: Adv.* **2**, 473 (2023)
35. D.N.H. Tran, S. Kabiri, T.R. Sim, D. Losic, *Environ. Sci.-Water Res.* **1**, 298 (2015)
36. T. Zhang, C. Xiao, J. Zhao, J. Cheng, K. Chen, Y. Huang, *ACS Omega* **4**, 7237 (2019)
37. L. Zhou, X. Zhao, G. Ju, *Adv. Mater. Interfaces Mater. Interfaces.* (2022). <https://doi.org/10.1002/admi.202101449>
38. Y. Fang, L. Yan, H. Liu, *A.C.S. Appl. Polym. Mater.* **2**, 3781 (2020)
39. J. Liu, L. Wang, F. Guo, L. Hou, Y. Chen, J. Liu, N. Wang, Y. Zhao, L. Jiang, *J. Mater. Chem. A* **4**, 4365 (2016)
40. C.F. Wang, S.J. Lin, *A.C.S. Appl. Mater. Interfaces* **5**, 8861 (2013)
41. Z. Wang, P. Jin, M. Wang, G. Wu, C. Dong, A. Wu, *A.C.S. Appl. Mater. Interfaces* **8**, 32862 (2016)

**Publisher's Note** Springer Nature remains neutral with regard to jurisdictional claims in published maps and institutional affiliations.

Springer Nature or its licensor (e.g. a society or other partner) holds exclusive rights to this article under a publishing agreement with the author(s) or other rightsholder(s); author self-archiving of the accepted manuscript version of this article is solely governed by the terms of such publishing agreement and applicable law.